Early Stages of ZnS Growth Studied by Stopped-Flow UV Absorption Spectroscopy: Effects of Educt Concentrations on the Nanoparticle Formation

ARTICLE *in* THE JOURNAL OF PHYSICAL CHEMISTRY B · DECEMBER 2006

Impact Factor: 3.3 · DOI: 10.1021/jp0638383 · Source: PubMed

4 AUTHORS:

Michael Tiemann
Universität Paderborn
83 PUBLICATIONS **2,035** CITATIONS
SEE PROFILE

Frank Marlow
Max Planck Institute for Coal Research
116 PUBLICATIONS **2,410** CITATIONS
SEE PROFILE

Felix J. Brieler
University of Hamburg
22 PUBLICATIONS **344** CITATIONS
SEE PROFILE

Mika Lindén
Universität Ulm
196 PUBLICATIONS **5,396** CITATIONS
SEE PROFILE

Early Stages of ZnS Growth Studied by Stopped-Flow UV Absorption Spectroscopy: Effects of Educt Concentrations on the Nanoparticle Formation

Michael Tiemann,*,† Frank Marlow,‡ Felix Brieler,§ and Mika Lindén*,§

Institut für Anorganische und Analytische Chemie, Justus-Liebig-Universität, Heinrich-Buff-Ring 58, D-35392 Giessen, Germany, Max-Planck-Institut für Kohlenforschung, Kaiser-Wilhelm-Platz 1, D-45470 Mülheim an der Ruhr, Germany, and Institutionen för Fysikalisk Kemi, Åbo Akademi, Porthansgatan 3-5, FIN-20500 Åbo, Finland

Received: June 20, 2006; In Final Form: September 10, 2006

The growth of ZnS nanoparticles by precipitation from supersaturated aqueous solution is studied by stopped-flow UV absorption spectroscopy. The average size, size distribution, and concentration of the particles are monitored within the sub-second time regime with a resolution of 1.28 ms. Particle growth at these early stages is governed by pronounced ripening. The UV absorption data strongly suggest that growth occurs by preferential adsorption of HS^- anions relative to Zn^{2+} or $ZnOH^+$ cations. Correspondingly, the initial sulfide concentration has a much more pronounced influence on the growth kinetics than the initial zinc concentration. These findings are verified by ζ-potential measurements which confirm that the particle surfaces are negatively charged under near-neutral pH conditions.

Introduction

The early stages of crystallization from solution and the mechanisms during subsequent crystal growth are increasingly attracting the attention of researchers from various fields. Deeper insight into fundamental processes during crystal growth is a challenge for chemists not just for academic reasons; a better understanding of the underlying principles may provide new opportunities to control the synthesis of solid materials and thus tailor the structural and physical properties of the products.[1,2] Modern analytical[3−9] and computational[10−14] techniques provide the opportunity to investigate even fast precipitation reactions from highly supersaturated solutions. A crucial point in these studies is the analytical access to inorganic chemical species with sizes in the range of a few nanometers. Such nanoparticles mark the boundary between molecules, which consist of a finite number of atoms, and macroscopic crystals, which contain virtually infinite numbers of atoms. They exhibit unique physical and chemical properties and are therefore of great interest in many fields, including fundamental research,[15−17] technology,[18,19] and even geophysics.[20]

The optical and electronic properties of small particles are strongly size-dependent and can therefore serve as a spectroscopic probe for the particle size. We have recently shown that it is possible to study the early stages of ZnS nanoparticle growth during precipitation from purely aqueous solution, that is, without capping ligands or other additives, by in-situ stopped-flow UV absorption spectroscopy.[9] We have developed a model for data analysis which comprises least-squares fits of the spectra, yielding both the energy and the intensity of the first excitonic band. This data treatment allows us not only to study the temporal evolution of the average particle size but also to follow changes in particle concentration. Here we present a more detailed analysis of the growth of sub-nanometer-sized ZnS particles in the 100-ms time regime, which takes into account unexpected educt concentration effects and their impact on the growth kinetics.

Experimental Section

Zinc sulfate monohydrate (99%, Fluka) and sodium sulfide nonahydrate (99%, Sigma) were used as received; water was purified (Millipore Academic A10). UV absorption spectroscopy was performed on an Applied Photophysics SX.18MV-R Stopped-Flow spectrometer equipped with a PDA.1 photodiode array detector and a UV.1 deuterium light source. Aqueous solutions of $ZnSO_4$ and Na_2S (10 μL each) were simultaneously injected into the observation cell (10-mm optical path length) from pressure-driven syringes; both the syringes and the observation cell were at a constant temperature of 293 K. The stopped-flow signal triggered the data acquisition with a dead time of approximately 2 ms; the first data used for analysis was at $t = 3.2$ ms. One hundred spectra were recorded within 127.4 ms, resulting in an integration time of 1.28 ms (= time resolution). All data were referenced against water. It was verified that the measurements were not influenced by deposition of ZnS on the observation cell windows; spectra of pure water showed identical zero absorption both before and after the experiment.

For data analysis the spectra were subjected to a least-squares fit deconvolution procedure, using three fully coupled Gaussian profile functions for the first three absorption bands as well as an exponential function. The energy of the first excitonic band is correlated with the particle radius r on the basis of the effective mass approximation,[21] assuming a finite potential model.[22] The integral intensity of the band is a relative measure for the particle concentration, assuming that the absorption cross section scales with r^3. Details on the data treatment are described in earlier work.[9]

The ζ-potential measurements were carried out on a Malvern Zetasizer Nano-ZS instrument equipped with a He−Ne laser.

* Corresponding authors. E-mail: (Tiemann) michael.tiemann@anorg.chemie.uni-giessen.de; (Lindén) mlinden@abo.fi.
† Justus-Liebig-Universität.
‡ Max-Planck-Institut für Kohlenforschung.
§ Åbo Akademi.

10.1021/jp0638383 CCC: $33.50
Published on Web 10/19/2006

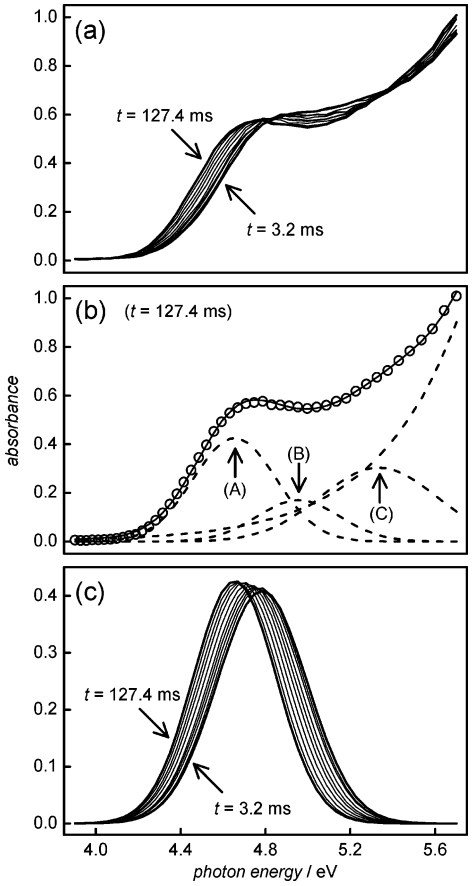

Figure 1. (a) Example of a time-resolved series of UV absorption spectra recorded within the first 127.4 ms of the formation of ZnS nanoparticles after mixing two aqueous precursor solutions ($[ZnSO_4]_0 = [Na_2S]_0 = 0.8$ mmol L^{-1}; for clarity, only 10 out of 100 spectra are considered). (b) Exemplified analysis of a spectrum by least-squares fitting of three fully coupled Gaussian and one exponential function.[9] The fit yields single absorption bands for the first excitonic transitions: (A) $E_{0,0}$, (B) $E_{0,0'}$, (C) $E_{1,0}$. (c) Temporal evolution of the first excitonic transition's absorption band; the shift of the peak maximum $E_{0,0}$ corresponds to the particle growth.

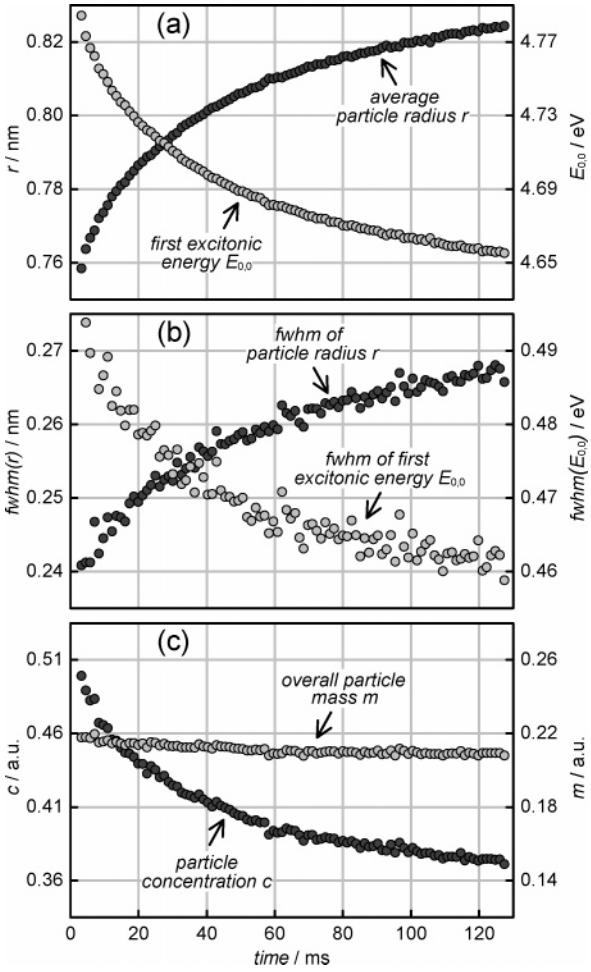

Figure 2. Temporal evolution of (a) the first excitonic transition's absorption energy $E_{0,0}$ and the corresponding average particle radius r according to eq 1, (b) the full width at half-maximum (fwhm) of the first excitonic transition's absorption energy $E_{0,0}$ and of the corresponding average particle radius r, and (c) the peak area $a_{0,0}$ of the first excitonic transition's absorption band which corresponds to the overall particle mass m (eq 3) and the corresponding particle concentration c according to eq 2 ($[ZnSO_4]_0 = [Na_2S]_0 = 0.8$ mmol L^{-1}).

Prior to each measurement, the $ZnSO_4$ and Na_2S solutions were mixed under vigorous stirring; 1 μL of the resulting mixture was then transferred into the measurement cell, which was at a constant temperature of 298 K. Each measurement, consisting of 20−30 runs, was repeated four times to obtain an average value.

Results

Figure 1a shows an example for a series of 100 spectra recorded within the first 127.4 ms after mixing aqueous solutions of $ZnSO_4$ and Na_2S (0.8 mmol L^{-1} each). A temporal shift of the absorption toward lower energy is obvious, which corresponds to the growth of the ZnS nanoparticles. Deconvolution of the spectra by least-squares fitting yields three Gaussian absorption bands corresponding to the first two excitonic transitions, as shown in Figure 1b for the last spectrum within the series. The fit procedure involves no more than a total of five independent variables.[9] Since the 1S-type electron holes are split into two components of slightly different energy (while the 1S-type states of the excited electrons remain degenerate),[23] the first excitonic transition leads to two absorption bands ($E_{0,0}$ and $E_{0,0'}$). For reasons of simplicity, we will neglect the splitting of the second excitonic band ($E_{1,0}$) here. Figure 1c shows the temporal evolution of the first band ($E_{0,0}$); from this band's absorption energy the average particle radius r can be calculated by[9]

$$r/\mathrm{nm} = \sqrt{\frac{1.236}{(E_{0,0} - E_g)/\mathrm{eV}}} - 0.290 \qquad (1)$$

where $E_g = 3.66$ eV is the bulk band gap energy. Figure 2a shows the temporal evolution of $E_{0,0}$, which decreases by about 0.13 eV within the measured time frame, as well as the resulting average particle radius r, which increases by about 0.07 nm. By first approximation the absorbance at the band's lower and upper borders at half-maximum corresponds to the respective borders in the particle radius distribution, assuming that polydispersity is the main reason for line broadening. As can be seen in Figure 2b, the full width at half-maximum (fwhm) of the particle radius increases with time, even though the absorption band narrows. This illustrates that line narrowing can easily be misinterpreted as particle-size focusing.

The area $a_{0,0}$ under the first excitonic transition's absorption band is proportional to the oscillator strength of the particles. The latter is strongly size dependent and scales with r^3.[9] Thus, the particle concentration can be described by

$$c \propto \frac{a_{0,0}}{r^3} \tag{2}$$

It follows that the peak area $a_{0,0}$ is proportional to the overall mass m of all particles (i.e., the mass of all precipitated material), as long as the particle volume is assumed to be proportional to r^3:

$$m \propto r^3 \cdot c \propto a_{0,0} \tag{3}$$

Figure 2c shows that the overall particle mass (peak area) changes only slightly during the studied time frame. Since this is within the assumed measurement errors, we can state that the overall mass remains approximately constant. However, the particle concentration decreases significantly by about 25%.

For a more comprehensive investigation of the ZnS nanoparticle formation we have varied the initial concentrations of the precursor solutions, $[ZnSO_4]_0$ and $[Na_2S]_0$, between 0.6 and 1.0 mmol L^{-1}. Figure 3a shows the temporal evolution of the average particle radii for stoichiometric (i.e., $[ZnSO_4]_0 = [Na_2S]_0$) as well as nonstoichiometric ($[ZnSO_4]_0 \neq [Na_2S]_0$) initial precursor concentrations. Figure 3b,c shows the respective changes in particle concentration and overall particle mass. The following trends are apparent and visualized in Figure 4. (i) Increasing $[Na_2S]_0$ while keeping $[ZnSO_4]_0$ constant leads to larger ZnS particle radii and higher particle concentrations. (ii) In the reverse case, that is, when $[ZnSO_4]_0$ is increased while $[Na_2S]_0$ is kept constant, smaller ZnS particles are obtained, but the particle concentration again increases; these latter two trends are weaker than those observed for varying $[Na_2S]_0$. (iii) The overall particle masses increase when either of the two components' initial concentration is raised; again, the effect is weaker for changes in $[ZnSO_4]_0$ than for $[Na_2S]_0$. The unexpected asymmetry with respect to the educts needs to be considered in detail in the Discussion section.

To obtain further insight into the particle growth we have carried out ζ-potential measurements in the aqueous dispersions of ZnS particles several minutes after mixing the precursor solutions. The properties of these "aged" dispersions may be different from those during our kinetic measurements, but ζ will at least qualitatively reflect the conditions during the early stages of particle growth. Figure 5 shows that ζ is negative in all systems, indicating negatively charged particle surfaces. This is to be expected for non-oxidized ZnS particles, since the reported isoelectric point (IEP) lies between 2.3 and 3.[24−27] A closer inspection of the results reveals some significant trends. (i) Increasing $[Na_2S]_0$ while keeping $[ZnSO_4]_0$ at a constant value leads to a substantial increase in the (negative) ζ potential; this is particularly pronounced as long as $[ZnSO_4]_0 \leq [Na_2S]_0$. (ii) The reverse case, that is, an increase in $[ZnSO_4]_0$ at a constant $[Na_2S]_0$, results in lower (negative) ζ values; however, this effect is less pronounced than that for changes in $[Na_2S]_0$, and it is almost negligible as long as $[ZnSO_4]_0 \geq [Na_2S]_0$. In all cases, the pH values lie between 7.2 and 7.5. Within this narrow range, a trend toward higher pH is observable for systems with high $[Na_2S]_0$, especially when $[ZnSO_4]_0 \leq [Na_2S]_0$.

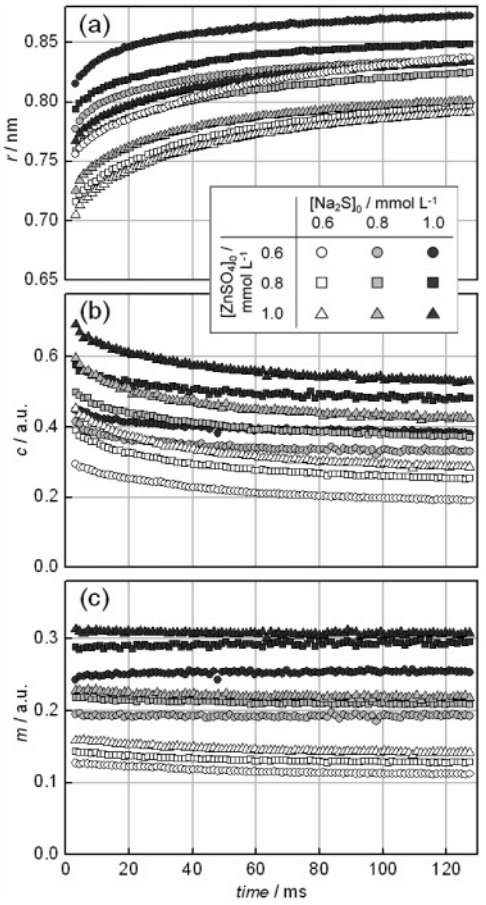

Figure 3. Temporal evolution of (a) the average particle radii r, (b) the particle concentrations c, and (c) overall particle masses m for various initial precursor concentrations. The symbol shape indicates the $ZnSO_4$ concentration (circles: $[ZnSO_4]_0 = 0.6$/squares: 0.8/triangles: 1.0 mmol L^{-1}) and the symbol color denotes the Na_2S concentration (white: $[Na_2S]_0 = 0.6$ mmol L^{-1}/gray: 0.8 mmol L^{-1}/black: 1.0 mmol L^{-1}).

Discussion

Ripening. According to the results in Figure 2, the growth of the ZnS particles (i.e., the increase of the average particle radius) is accompanied by a substantial decrease in particle concentration, while the overall mass of precipitated material is approximately constant. This is clearly indicative of ripening, that is, growth of larger particles at the expense of smaller ones. The assumption of ripening is also consistent with the fact that an increase in the initial precursor concentrations tends to result in larger average particle sizes (see Figure 3). A higher precursor concentration (i.e., a higher degree of supersaturation) is expected to create a larger number of nuclei; without ripening, this would lead to a higher particle concentration, but usually not to larger particles.

The general term "ripening" refers basically to either of two potential mechanisms. (i) "Ostwald ripening" corresponds to the dissolution of small particles (which in nanoparticulate systems are often more soluble than larger ones), followed by their reprecipitation at the surface of larger particles. (ii) Alternatively, the phenomenon of ripening may occur by "coalescence", that is, the merger of two particles into one larger particle. For crystalline particles, coalescence is often more comprehensively described by the concept of "oriented attachment",[28] which takes into account that, after colliding, the two merging particles need to take up suitable crystallographic orientation by rotational movement relative to each other. On the basis of our data, it is not possible to unambiguously discriminate between the two ripening mechanisms, that is, Ostwald ripening and/or coalescence. The ζ-potential measurements suggest that the repulsive forces between the particles are low enough to allow for coalescence to occur; stabilization of dispersed particles by electrostatic repulsion usually requires ζ-values higher than about 30 mV.[29] In theory, a comparison

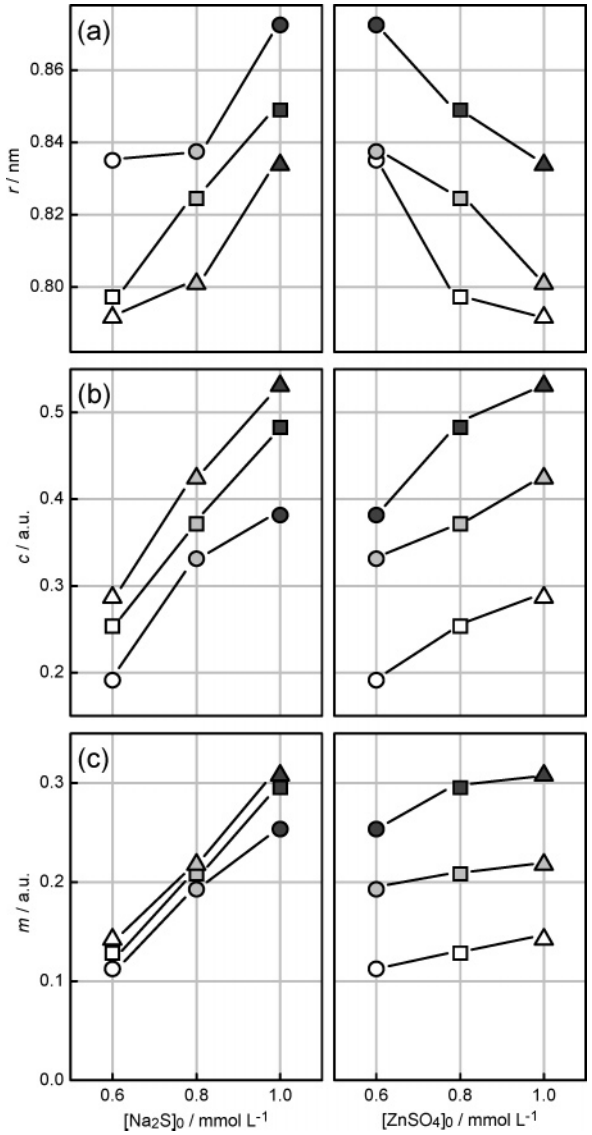

Figure 4. (a) Average particle radii *r*, (b) particle concentrations *c*, and (c) overall particle masses *m* after 127.4 ms for various initial precursor concentrations. To better visualize the impact of changing either of the two components' initial concentrations, the data are plotted against both $[Na_2S]_0$ (left) and $[ZnSO_4]_0$ (right); for the legend, see Figure 3.

of the experimental data to the respective kinetic models which describe the two mechanisms would answer this question. However, such models can only be approximations of rather complex kinetics. Both mechanisms may contribute to particle growth, and mixing inhomogenities may distort the earliest stages of growth to some degree. Therefore, kinetic studies will usually fail to deliver unambiguous proof for one particular mechanism. Furthermore, simple kinetic models may not be suitable for our system, since the particles turn out to be nonstoichiometric, as we will discuss in the following. Nevertheless, independent of the actual mechanism, we can state that the particle growth in our system is clearly governed by pronounced ripening; this observation will be of significance in the subsequent interpretation of our data (see below: Growth Model).

Particle Surface Charge. The simplest model for the formation of ZnS nanoparticles from aqueous solutions of $ZnSO_4$ and Na_2S is that the ZnS particles have a strictly stoichiometric composition of Zn/S = 1 at any time and that

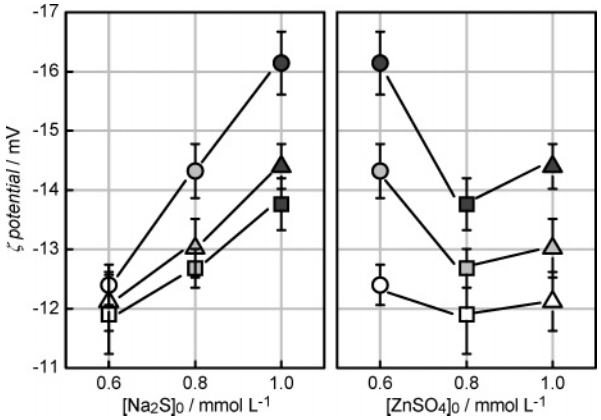

Figure 5. The ζ-potentials measured in aqueous dispersions of ZnS particles several minutes after mixing the precursor solutions with various concentrations. For clarity, the data are plotted against both $[Na_2S]_0$ (left) and $[ZnSO_4]_0$ (right); for the legend, see Figure 3.

precipitation occurs quantitatively, since the solubility of ZnS is extremely low.[30] The final amount of precipitated material would then have to be proportional to the initial concentration of the precursors or (in the case of nonstoichiometric precursor concentrations) to that of the less concentrated precursor. Thus, the overall ZnS particle masses in Figure 3c would have to converge to the same values as long as one of the two components' initial concentration is kept constant. However, this simple model clearly does not apply to our system. In Figure 3c, all overall masses apparently reach approximately constant values at the end of the runs (after ca. 100 ms), but do not follow the above predictions. In fact, higher initial precursor concentrations lead to a more-than-proportional increase in the overall particle masses, and the latter do not converge to the same values when the initial concentration of one component is fixed (see Figure 4). As pointed out in the Results section, this more-than-proportional behavior is more pronounced for changes in $[Na_2S]_0$ than in $[ZnSO_4]_0$.

The finding that varying $[Na_2S]_0$ affects the ZnS particle radius and concentration much more than $[ZnSO_4]_0$ is a strong indication that particle growth requires more than one equivalent of sulfide for each zinc. This may apply to the event of particle nucleation as well as to later stages of ZnS nanoparticle growth. The former aspect, that is, the occurrence of Zn/S ratios lower than one during nucleation, is consistent with experimental investigations[31] as well as simulation studies[14,32] which indicate the existence of several zinc-deficient species, such as $(Zn_2S_3)^{2-}$, $(Zn_4S_6)^{4-}$, $(ZnS_2)^{2-}$, or $(ZnS_3)^{4-}$, which seem to play a major role during the nucleation of ZnS in supersaturated solution. It is therefore likely that an excess supply of sulfur with respect to zinc facilitates nucleation, resulting in a higher concentration of particles, which is what we observe in our data.

However, apart from the instant of nucleation, the occurrence of Zn/S ratios lower than one is also plausible for later stages in ZnS nanoparticle growth. Even when we assume that very small ZnS nanoparticles already resemble the bulk crystal structure (zinc blende, i.e., sphalerite),[33] a stoichiometric Zn/S ratio can be postulated only for the core region of the particles. The surface region, on the other hand, may be locally nonstoichiometric. Since very small particles have high surface-to-volume ratios, a relative excess of sulfide at the particle surface would have a strong effect on the overall stoichiometry. The radii of the ZnS particles in our study lie below 1 nm, which means that they consist of barely more than 100 atoms. In theory, a ZnS particle with six shells of ions (around one central sulfide ion) has a radius of 0.885 nm (which is the maximum

of what we observe) and consists of 147 ions;[34] 64 of these ions (43%) are located at the surface, which illustrates how significantly a nonstoichiometric composition of the surface will render the overall Zn/S ratio nonstoichiometric, too. Hence, we conclude that the surface of our ZnS nanoparticles contains more sulfur than zinc. The particles should therefore more accurately be noted as "$(Zn_xS_{x+y})^{2y-}$".

The ζ-potential measurements support the assumption that the ZnS particles carry more sulfide than zinc at the surface. For ZnS, the potential-determining ions have been shown to be H^+, OH^-, HS^-, Zn^{2+}, and $ZnOH^+$.[24] However, the pH some minutes after precipitation is in a narrow range of 7.2−7.5 under the applied experimental conditions, which means that the differences in the H^+ and OH^- concentrations are much too small to explain the significant changes in the ζ-values, especially as ZnS has a remarkable plateau behavior in the neutral pH range.[24] Thus, the behavior of the ζ-values must be ascribed to changes in the concentrations of HS^-, Zn^{2+}, and $ZnOH^+$. As pointed out in the Results section, an increase in $[Na_2S]_0$ at a constant $[ZnSO_4]_0$ results in a significantly higher (negative) ζ-value, indicating that more sulfide is adsorbed to the particle surface when more sulfide is available in solution. An increase in $[ZnSO_4]_0$ at a constant $[Na_2S]_0$, on the other hand, has a much lower impact (i.e., a less significant decrease of the negative ζ-value), confirming that a higher zinc concentration in solution will not result in pronounced Zn^{2+} or $ZnOH^+$ adsorption. Note that the most negative ζ-value was measured at the highest level of Na_2S excess, where electrostatic screening of additional ions present in solution would be expected to decrease the absolute value of the ζ-potential. In theory, the correlation between ζ and $[Na_2S]_0$ might also be a pH-related effect. An increase in $[Na_2S]_0$ leads to a higher pH owing to the strong basicity of sulfide according to the equilibrium in eq 4 which lies far on the right-hand side:[30]

$$S^{2-} + H_2O \leftrightarrows SH^- + OH^- \quad (4)$$

However, as pointed out above, this pH shift is very weak and cannot account for the significant correlation between ζ and $[Na_2S]_0$. Thus, the latter must be the result of preferential HS^- adsorption. This is in agreement with reports in the literature for aqueous ZnS dispersions in the presence of $(NH_4)_2S$ as an additional sulfide source under oxygen-free conditions.[24] Our measurements were not carried out under oxygen-free conditions, which is why there is a theoretical possibility for the formation of ZnO. However, we believe that this effect is negligible in our case. Powder X-ray diffraction (XRD) analysis of the precipitate (see Supporting Information) confirms that no significant quantities of ZnO are formed; all diffraction peaks correspond to cubic zinc blende ZnS. (Applying Scherrer's formula to the powder XRD pattern suggests a particle radius between 1.1 and 1.2 nm, which is a little larger than the value of 0.82 nm obtained from the UV data after 127 ms, see Figure 2. Given the fact that isolating and drying the material for XRD analysis required several hours, it is to be expected that further particle growth has occurred, which is why the particle sizes obtained from XRD and UV studies may be regarded as consistent with each other.) More importantly, if ZnO formation played a significant role, we would expect an IEP value closer to that of ZnO, which, according to the literature, lies between 8.6 and 9.8,[27] that is, our ζ- values would have to be positive, which is not the case. Finally, we observe a logical trend in our results, and especially under excess sulfide conditions we should have a more reducing rather than oxidizing environment. Thus, we conclude that HS^- is adsorbing much more strongly than either Zn^{2+} or $ZnOH^+$ to the ZnS surface under our experimental conditions. In summary, both the in-situ UV absorption data and the ζ-potential measurements provide indirect, yet strong evidence for a nonstoichiometric surface composition of the growing particles. Given the very short time frame of this study, direct determination of the stoichiometry, such as by XPS, is not possible. Subsequent analysis of the stoichiometry in the precipitated material by ex-situ analysis will hardly reflect the conditions present during the early stages of particle growth.

Growth Model. We can now comprehend the results from the kinetic measurements. The Zn/S ratio in our particles is generally smaller than one, owing to the excess sulfide at the particle surface. Therefore, the Zn/S ratio of the particles depends necessarily quite significantly on the particle radius. The larger the particles get, the lower will be the surface-to-volume ratio; thus, Zn/S will increase and eventually converge to 1 when the particle radius reaches infinity. As a consequence, the precursor concentrations in solution will develop in the opposite way. Due to the sulfide excess of the particles, the Zn/S ratio in solution will always be greater than its initial value, $[ZnSO_4]_0/[Na_2S]_0$, but it will gradually decrease and eventually converge to that value while the particle radius increases. In this way we can explain why higher initial precursor concentrations lead to more-than-proportionally higher final overall particle masses, The actual reason is related to the observation that higher initial precursor concentrations always result in larger particle radii, owing to ripening, as discussed above (see Figure 3). Thus, the sulfur deficiency in solution is lower, which, in turn, means that a larger fraction of the precursors are consumed in the particle formation and growth.

Conclusions

We have shown that the early stages of ZnS nanoparticle growth by precipitation from supersaturated aqueous solution is governed by ripening processes both for stoichiometric and for nonstoichiometric educt concentrations. This is apparent from the fact that the increase in average particle size is accompanied by a substantial decrease in particle concentration. The growing particles have negatively charged surfaces, due to preferential adsorption of HS^-. The Zn/S ratio at the surface and, owing to the high surface-to-volume ratio, in the overall composition of the particles is therefore lower than one. Correspondingly, the initial sulfide concentration has a much more pronounced influence on the growth kinetics than the initial zinc concentration.

Acknowledgment. We thank Juha Hartikainen (Åbo Akademi) for his help and input. Part of this work was funded by the European Union project "Atomic Level Studies of Solids Nucleation and Reactions (NUCLEUS, HPRN-CT-1999-00025) and by the Finnish Academy of Sciences. M.T. thanks Prof. Michael Fröba for continuous support.

Supporting Information Available: Powder X-ray diffraction (XRD) diagrams of the ZnS precipitate and of ZnS (zinc blende)/ZnO as references. This material is available free of charge via the Internet at http://pubs.acs.org.

References and Notes

(1) Schüth, F. *Curr. Opin. Solid State Mater. Sci.* **2001**, *5*, 389−395.
(2) Schüth, F.; Bussian, P.; Ågren, P.; Schunk, S.; Lindén, M. *Solid State Sci.* **2001**, *3*, 801−808.
(3) Fischer, C.-H.; Weller, H.; Fojtik, A.; Lume-Pereira, C.; Janata, E.; Henglein, A. *Ber. Bunsen-Ges. Phys. Chem.* **1986**, *90*, 46−49.

(4) Nosaka, Y.; Ohta, N.; Fukuyama, T.; Fujii, N. *J. Colloid Interface Sci.* **1993**, *155*, 23−29.
(5) Meneau, F.; Sankar, G.; Morgante, N.; Winter, R.; Catlow, C. R. A.; Greaves, G. N.; Thomas, J. M. *Faraday Discuss.* **2002**, *122*, 203−210.
(6) Meneau, F.; Cristol, S.; Sankar, G.; Dolbnya, I. P.; Bras, W.; Catlow, C. R. A.; Thomas, J. M.; Greaves, G. N. *J. Appl. Crystallogr.* **2003**, *36*, 718−721.
(7) Bullen, C. R.; Mulvaney, P. *Nano Lett.* **2004**, *4*, 2303−2307.
(8) Qu, L.; Yu, W. W.; Peng, X. *Nano Lett.* **2004**, *4*, 465−469.
(9) Tiemann, M.; Weiss, Ö.; Hartikainen, J.; Marlow, F.; Lindén, M. *ChemPhysChem* **2005**, *6*, 2113−2119.
(10) Rein ten Wolde, P.; Frenkel, D. *Phys. Chem. Chem. Phys.* **1999**, *1*, 2191−2196.
(11) Auer, S.; Frenkel, D. *Nature* **2001**, *409*, 1020−1023.
(12) Ojo, S. A.; Whitmore, L.; Slater, B.; Catlow, C. R. A. *Solid State Sci.* **2001**, *3*, 821−826.
(13) Talapin, D. V.; Rogach, A. L.; Haase, M.; Weller, H. *J. Phys. Chem. B* **2001**, *105*, 12278−12285.
(14) Hamad, S.; Cristol, S.; Catlow, C. R. A. *J. Am. Chem. Soc.* **2005**, *127*, 2580−2590.
(15) Alivisatos, A. P. *J. Phys. Chem.* **1996**, *100*, 13226−13239.
(16) Eychmüller, A. *J. Phys. Chem. B* **2000**, *104*, 6514−6528.
(17) Bukowski, T. J.; Simmons, J. H. *Crit. Rev. Solid State Mater. Sci.* **2002**, *27*, 119−142.
(18) Bhattacharya, P.; Ghosh, G.; Stiff-Roberts, A. D. *Annu. Rev. Mater. Res.* **2004**, *34*, 1−40.
(19) Skolnick, M. S.; Mowbray, D. J. *Annu. Rev. Mater. Res.* **2004**, *34*, 181−218.
(20) Labrenz, M.; Druschel, G. K.; Thomsen-Ebert, T.; Gilbert, B.; Welch, S. A.; Kemner, K. M.; Logan, G. A.; Summons, R. E.; De Stasio, G.; Bond, P. L.; Lai, B.; Kelly, S. D.; Banfield, J. F. *Science* **2000**, *290*, 1744−1747.
(21) Brus, L. E. *J. Chem. Phys.* **1983**, *79*, 5566−5571.
(22) Nosaka, Y. *J. Phys. Chem.* **1991**, *95*, 5054−5058.
(23) Chestnoy, N.; Hull, R.; Brus, L. E. *J. Chem. Phys.* **1986**, *85*, 2237−2242.
(24) Nicolau, Y. F.; Menard, J. C. *J. Colloid Interface Sci.* **1992**, *148*, 551−570.
(25) Williams, R.; Labib, M. E. *J. Colloid Interface Sci.* **1985**, *106*, 251−254.
(26) Pugh, R. J.; Tjus, K. *J. Colloid Interface Sci.* **1987**, *117*, 231−241.
(27) Kosmulski, M. *Chemical Properties of Material Surfaces*; CRC Press: Boca Raton, FL, 2001.
(28) Penn, R. L. *J. Phys. Chem. B* **2004**, *108*, 12707−12712.
(29) Brinker, C. J.; Scherer, G. W. *Sol−Gel Science*; Academic Press: New York, 1990; p 243.
(30) Myers, L. J. *J. Chem. Educ.* **1986**, *63*, 687−690.
(31) Luther, G. W.; Theberge, S. M.; Rickard, D. T. *Geochim. Cosmochim. Acta* **1999**, *63*, 3159−3169.
(32) Hamad, S.; Catlow, C. R. A.; Spanó, E.; Matxain, J. M.; Ugalde, J. M. *J. Phys. Chem. B* **2005**, *109*, 2703−2709.
(33) Zhang, H.; Gilbert, B.; Huang, F.; Banfield, J. F. *Nature (London)* **2003**, *424*, 1025−1029.
(34) Lippens, P. E.; Lanoo, M. *Phys. Rev. B* **1989**, *39*, 10935−10942.